https://ntrs.nasa.gov/search.jsp?R=19700019512 2020-03-12T02:01:30+00:00Z

N 70 28822
NASA CR 101198

THEORETICAL CHEMISTRY INSTITUTE

THE UNIVERSITY OF WISCONSIN

NGL-50-002-001

PERMEABILITY OF A ONE-DIMENSIONAL POTENTIAL BARRIER

by

R. J. Le Roy, K. A. Quickert and D. J. Le Roy

WIS-TCI-384

March 31, 1970

CASE FILE
COPY

MADISON, WISCONSIN

Permeability of a One-Dimensional Potential Barrier

by

R. J. Le Roy

Theoretical Chemistry Institute and Chemistry Department,
University of Wisconsin, Madison, Wisconsin 53706

and

K. A. Quickert[§] and D. J. Le Roy

Lash Miller Chemical Laboratories, University of Toronto
Toronto 181, Ontario, Canada

ABSTRACT

A numerical method is described for computing the exact permeability (tunneling probability) for any one-dimensional potential barrier. It is used to test the validity of the widely used approximate formulae for the tunneling factors for truncated parabolic barriers. The method is also used to calculate tunneling factors for the $H+H_2$ exchange reaction, using the theoretical potential surface of Shavitt, Stevens, Minn, and Karplus, and it is shown that standard Eckart and parabolic barrier approximations can yield considerable error.

[§]Present address: Institut für Physikalische Chemie,
Universität Göttingen,
34 Göttingen, Bürgerstrasse 50,
West Germany.

Evaluation of the probability of transmission for a particle impinging on a potential barrier has long been an important problem in the theoretical treatment of chemical reaction rates. The early use of tunneling corrections is discussed by Glasstone, Laidler, and Eyring.[1] Their usefulness in interpreting the results of proton transfer reactions has recently been reviewed by Caldin,[2] and their application to the hydrogen exchange reactions is discussed by Johnston.[3]

While the potential barrier in a chemical reaction is in general multi-dimensional, a very widely used approximation has been to consider the reaction as motion along a one-dimensional (1-Dim) "reaction path" which is orthogonal to all other modes of motion of the interacting species. In this approximation, estimates of barrier transmission rates have usually been obtained after approximating the exact potential by a model 1-Dim barrier of one of two analytic forms for which exact analytic tunneling probabilities are known: an Eckart barrier,[4] or an infinite parabolic barrier.[5] An exact tunneling probability expression has also recently been derived[6] for a third potential form, the infinite double anharmonic barrier, $V(x) = V_o[1 - (x/a - a/x)^2]$; however, this result has not yet been applied to chemical problems. Although the result for the parabolic potential is for an infinite barrier, it has been widely used for truncated parabolas,[2] probably largely because of the very convenient analytic expression obtained for the tunneling factor in the high temperature limit.[7] The Eckart potential,[4] on the other hand, is finite, and the potential and its first derivative are everywhere continuous; however, while its exact transmission probability is known analytically, the tunneling factor cannot be obtained in closed

form.*

---

* A table of Eckart tunneling factors for a wide range of potential parameter values and reduced temperatures is given in Ref. 3. (p. 44). Johnston (private communication, 1969) computed this table using the correct transmission probability expression and not his[3] Eq. (2-22), in which the last term should be $\pi^2/4$, not $2\pi^2/16$.

Despite the convenience of using the analytic[7] or tabulated[3] results for the two main model barriers mentioned above, these potentials will very rarely accurately represent a reasonable 1-Dim cut through an actual potential surface. Furthermore, the analytic tunneling probabilities can in no way take account of the change in the asymptotic reduced mass between reagents and products which arises in many chemical situtations. An additional problem associated with the use of Bell's formulae[7] for parabolic barriers is the unknown effect of truncating the barrier at a finite height on the transmission coefficient, and hence on his approximate expressions for the tunneling factor.

In the next section, a simple numerical procedure is presented for determining exact transmission coefficients for any 1-Dim potential barrier. This approach is tested by comparing its predictions to the exact analytic result for an Eckart barrier.[4] The numerical method is then applied to truncated parabolic barriers to examine the validity of Bell's approximations. Finally, the usefulness of the exact 1-Dim method is demonstrated by applying it to the calculation of tunneling factors for the $H+H_2$ exchange reaction.

SCATTERING BY A 1-DIM BARRIER

Exact Barrier Passage Probability

Many elementary quantum mechanics texts derive the exact transmission probability for the case of a rectangular barrier,[8] and the present treatment is qualitatively exactly the same. The Schrödinger equation describing 1-Dim potential scattering may be written in the dimensionless form

$$\frac{d^2}{dy^2}\psi(y) + B_y\,[\overline{E}-\overline{V}(y)]\,\psi(y) = 0\ , \qquad (1)$$

where $y = x/a$, $\overline{E} = E/V_o$, $\overline{V}(y) = V(x)/V_o$, and

$$B_y = 2\mu V_o a^2/\hbar^2 = 20.74659\ \mu[\text{amu}]\ V_o[\text{kcal/M}]\ (a[\text{Å}])^2\ .$$

In general, the energy and length scaling factors V_o and a may be chosen completely arbitrarily; however it is usually convenient to associate them with the barrier height and width. In the present discussion, the coordinate x along the reaction path is defined such that $x \sim -\infty$ corresponds to reagents and $x \sim +\infty$ to products. The potential $V(x)$ is everywhere finite and approaches constant values in the limits $x \sim \pm\infty$ (see Fig. 1). E is the energy of the incoming particle; in general its effective reduced mass μ may vary along the reaction coordinate, and the asymptotic reduced mass of the reagents may differ with that of the products.[9] However, this may readily be taken account of by simply introducing a variable mass $\mu = \mu(y)$ into Eq. (1), or

alternately by scaling the reaction coordinate appropriately while holding μ fixed.[10] When this question arose here the latter approach was used, and hence μ is assumed to be a constant in the rest of the derivation.

For "reagents", the solutions of Eq. (1) may be asymptotically expressed as a linear combination of plane waves incident on and reflected from the barrier; i.e., for $y \sim -\infty$:

$$\psi(y) = A_I e^{i\alpha_1 y} + A_R e^{-i\alpha_1 y} \tag{2}$$

where $\alpha_1 = (B_y)^{1/2} [\bar{E}-\bar{V}(-\infty)]^{1/2}$. Similarly, particles which tunnel past the barrier to form products may be described asymptotically by a plane wave moving away from the barrier; i.e., for $y \sim +\infty$:

$$\psi(y) = A_T e^{i\alpha_2 y} \tag{3}$$

where $\alpha_2 = (B_y)^{1/2} [\bar{E} - \bar{V}(+\infty)]^{1/2}$. The probability of barrier passage is clearly the ratio of the transmitted to the incident flux:

$$\kappa(\bar{E}) = \frac{v_+}{v_-} \left|\frac{A_T}{A_I}\right|^2$$

where v_+ and v_- are respectively the asymptotic velocities of products (+) and reagents (-). For fixed μ, $v_+/v_- = \alpha_2/\alpha_1$, and hence

$$\kappa(E) = \frac{\alpha_2}{\alpha_1} \left|\frac{A_T}{A_I}\right|^2 \tag{4}$$

To facilitate computation of $\kappa(\bar{E})$ it is convenient to expand $\psi(y)$ in terms of its real and imaginary parts:

$$\psi(y) = \phi_1(y) + i\,\phi_2(y)$$

Comparing this with Eq. (3) shows that for products, at $y \sim +\infty$:

$$\begin{aligned} \phi_1(y) &= A_T \cos(\alpha_2 y) \\ \phi_2(y) &= A_T \sin(\alpha_2 y) \end{aligned} \tag{5}$$

Starting from this boundary condition with an arbitrary choice of A_T (most conveniently, $A_T \equiv 1$), the two independent solutions $\phi_1(y)$ and $\phi_2(y)$ may be numerically integrated back through the barrier to the reagent boundary condition at $y \sim -\infty$. There they may readily be decomposed into

$$\begin{aligned} \phi_1(y) &= C_1 \cos(\alpha_1 y) + D_1 \sin(\alpha_1 y) \\ \phi_2(y) &= C_2 \cos(\alpha_1 y) + D_2 \sin(\alpha_1 y) \quad . \end{aligned} \tag{6}$$

Comparing equations (2) and (6), values of A_I and A_R are readily obtained in terms of values of the solution functions $\phi_1(y)$ and $\phi_2(y)$ at the adjacent integration mesh points y_1 and y_2. Substituting them into Eq. (4) yields

$$\begin{aligned} \kappa(\bar{E}) = 4(\alpha_2/\alpha_1) \sin^2[\alpha_1(y_2-y_1)]\,|A_T|^2 \Big\{ & [\phi_1(y_1)]^2 \\ & + [\phi_1(y_2)]^2 + [\phi_2(y_1)]^2 + [\phi_2(y_2)]^2 \\ & - 2[\phi_1(y_1)\,\phi_1(y_2) + \phi_2(y_1)\phi_2(y_2)]\cos[\alpha_1(y_2-y_1)] \\ & + 2[\phi_1(y_1)\,\phi_2(y_2) - \phi_1(y_2)\phi_2(y_1)]\sin[\alpha_1(y_2-y_1)] \Big\}^{-1} . \end{aligned} \tag{7}$$

This is the desired result. The exact numerical integration of Eq. (1) and the practical application of the boundary conditions are discussed below.

The above method was tested by applying it to a symmetric Eckart barrier, $\bar{V}(y) = 1./\cosh^2(y)$, for which the exact $K(\bar{E})$ function is known analytically.[4] For barriers with B_y values ranging from 2 to 200, it was found that single precision numerical integration yielded $K(\bar{E})$ accurate to within $1.\times10^{-5}$, for $\bar{E} = 0.1$, 1.0, and 2.0. This confirms the validity of the present approach.

Integration of Eq. (1) and Application of Boundary Conditions

The Numerov method[11] is known to be a very efficient algorithm for the numerical integration of a homogeneous linear second-order differential equation without first derivatives, such as Eq. (1).[12] One restriction on its use is that it assumes that the potential function $\bar{V}(y)$ is smooth, since when it is not an inordinately small increment of integration is required to yield reasonable accuracy. In the latter situation a lower-order algorithm such as the Runge-Kutta-Gill (RKG) method[13] is more appropriate. The RKG procedure requires more arithmetic, and one more function evaluation per integration step than does the Numerov method. However, when calculating the solution at a given point the latter utilizes the solution at the two previous mesh points, while the former requires the solution and its first derivative only at the adjacent previous point. Thus, if RKG is used and the integration mesh chosen so that mesh points lie at any potential slope discontinuities, the numerical integration is in no way affected by the existence of such discontinuities. In the

present work, the RKG procedure was used in the calculations for truncated parabolic barriers, as they have discontinuous first derivatives at $y = \pm 1$ (see below). The Numerov method was used in all other cases.

For either algorithm the accuracy of the integration improves with decreasing increment dy until a lower bound is reached beyond which the theoretical improvement in the numerical accuracy is exceeded by the accumulated machine round-off error. The optimum increment of integration as a function of particle and barrier size is approximately given by

$$dy = dx/a = F/(B_y)^{1/2} ,$$

where B_y is as defined above with V_o being the height of the barrier. The value of the numerical constant F depends on the integration algorithm and the number of significant digits of machine accuracy. On the 8-digit computer used in the present work, $F = 0.18$ was found to be appropriate for Numerov integration, and $F = 0.07$ for the RKG algorithm.

For potentials with a finite range, such as truncated parabolic barriers, application of the boundary conditions Eqs. (2) and (3) presents no difficulties. On the other hand, realistic potentials which reach their asymptotic values only in the limits $y \sim \pm \infty$ can only be integrated over a finite interval, and hence the exact boundary conditions are never quite achieved. In the present work, the ends of this finite interval, y_- and y_+, were defined as the smallest values of $|y|$ for which the first-order WKB convergence criterion was smaller than a chosen critical value. Thus, they are the solutions of

$$\left| [\alpha(y)]^{-2} \frac{d}{dy} \alpha(y) \right| = Z$$

where $\alpha(y) = (B_y)^{1/2} [\bar{E}-\bar{V}(y)]^{1/2}$ and Z is the chosen convergence criterion. It was found here that $Z = 1.0\times10^{-5}$ yielded values of $\kappa(\bar{E})$ within 1×10^{-5} of the exact analytic barrier passage probabilities for Eckart barriers of different sizes.

A Fortran listing of the subroutine used to integrate Eq. (1) to yield $\kappa(\bar{E})$ is given in the Appendix to Ref. 14.

The Tunneling Factor $\Gamma(T)$

The tunneling factor is the ratio of the quantum mechanical to the classical barrier-crossing rate for particles with a Boltzman distribution of initial kinetic energies relative to the barrier. In reduced units analogous to those of Eq. (1), it may be written as[3]

$$\Gamma(\bar{T}) = (1/\bar{T})\, e^{(1/\bar{T})} \int_0^\infty \kappa(\bar{E})\, e^{-\bar{E}/\bar{T}}\, d\bar{E} \qquad (8)$$

where $\bar{T} = kT/V_o$, and V_o is the barrier height. After obtaining $\kappa(\bar{E})$ values over a range of energies by the method presented above, Eq. (8) may be integrated numerically. This quantity is in effect an observable and is the point of comparison between theoretical and experimental estimates of tunneling.

APPLICATION TO PARABOLIC BARRIERS

The potential form which appears to have been most widely used to account for tunneling in chemical processes[2] is the truncated parabola:

$$\begin{aligned} \bar{V}(y) &= 1 - y^2 \qquad \text{for} \quad -1 \le y \le 1 \\ &= 0 \qquad\quad \text{for} \quad |y| > 1 \quad , \end{aligned} \qquad (9)$$

where particles may impinge on the barrier with energies $\bar{E} > 0$. In the present discussion, the energy and length scaling factors V_o and a always signify the barrier height, and half-width at its base. It is apparent that in this case the transmission probability function $\kappa(\bar{E})$ is completely defined by the corresponding value of B_y, since Eq. (1) is precisely the same for all barriers with different heights and widths, but the same B_y.

It will be convenient from this point on to replace B_y by the previously used,[2,7] entirely equivalent reduced parameter

$$\beta = \pi\,(B_y)^{1/2} = 14.30946\,\left(\mu[\text{amu}]\; V_o[\text{kcal/M}]\right)^{1/2}\; a[\text{Å}]$$

$$= 2197.524\; V_o[\text{kcal/M}]\;/\;\nu[\text{cm}^{-1}]\quad ,$$

where ν is the characteristic frequency of the harmonic oscillator potential obtained on inverting the parabolic barrier.†

---

† While consideration of Eq. (1) suggests that B_y is a more "natural" parameter, previous work with truncated parabolas[2,7] used β, which is a natural parameter in Bell's[7] approximate analytic tunneling factor expressions.

It should also be noted that the reduced temperature $\bar{T}$ used here is entirely equivalent to the previously used reduced variable $\alpha = 1/\bar{T}$. In the following discussion particular combinations of temperature, and particle mass and barrier size are characterized by values of $\bar{T}$ and β. For given choices of these quantities, exact values of $\kappa(\beta,\bar{E})$ and $\Gamma(\beta,\bar{T})$ were calculated by the numerical method presented above.

It is well known[5] that the exact transmission probability for particles impinging on an infinite parabolic barrier: $\overline{V}(y) = 1 - y^2$, where $-\infty < y < +\infty$, is

$$\kappa_\infty(\beta,\overline{E}) = \left\{1 + \exp[\beta(1 - \overline{E})]\right\}^{-1} \tag{10}$$

where $\overline{E}$ and β are as defined above, and in general $\overline{E}$ may range to $\pm\infty$. A widely used approximation has been to assume that the transmission coefficient for a finite parabolic barrier may be accurately represented by Eq. (10). This question is examined in Fig. 2 where the ratios of approximate (from Eq. (10)) to exact numerical (κ_{ex}) transmission coefficients are plotted against $\overline{E}$ for barriers of different sizes (different β's). It is apparent that the error inherent in the use of $\kappa_\infty(\beta,\overline{E})$ for finite barriers increases with decreasing β, and that for the particle and barrier sizes considered, Eq. (10) becomes satisfactory only for energies above the top of the barrier ($\overline{E} = 1$). However, in all cases it is significantly in error at low values of $\overline{E}$, and this will effect the tunneling factors at low temperatures.

Bell's[7] widely used formulae for the tunneling factors for truncated parabolic barriers are based on Eq. (10). On substituting it into Eq. (8) he obtained an analytic approximation for the resulting integral, yielding

$$\Gamma_\infty^{\,I}(\beta,\overline{T}) = \frac{\pi/\beta\overline{T}}{\sin(\pi/\beta\overline{T})} - \frac{\exp(1/\overline{T}-\beta)}{\beta\overline{T}-1}\left\{1 - \left(\frac{1-\beta\overline{T}}{1-2\beta\overline{T}}\right)e^{-\beta} + \left(\frac{1-\beta\overline{T}}{1-3\beta\overline{T}}\right)e^{-2\beta} - \ldots\right\}. \tag{11}$$

Although individual terms in this expansion have singularities at integer values of $1/\beta\bar{T}$, there is exact mutual cancellation of such terms so that the sum remains finite and Eq. (11) is defined for all values of $\beta\bar{T}$.**

** In Bell's original treatment[7] he unnecessarily[2] restricted the use of Eq. (11) to $\beta\bar{T} > 1$.

Bell also noted[7] that in the high temperature region where

$$\left| \frac{\exp(1/\bar{T}-\beta)}{\beta\bar{T}-1} \right| << 1 \quad ,$$

$\Gamma_{\infty}^{I}(\beta,\bar{T})$ becomes

$$\Gamma_{\infty}^{II}(\beta,\bar{T}) = \frac{\pi/\beta\bar{T}}{\sin(\pi/\beta\bar{T})} \quad , \tag{12}$$

which has been used widely.[2,9] The accuracies of these approximate formulae are illustrated in Fig. 3, where their predictions are compared to the exact numerical values $\Gamma_{ex}(\beta,\bar{T})$; the solid curves used Eq. (11) for Γ_{∞}, and the broken curves Eq. (12). The breaks in the solid curves at integer values of $1/\beta\bar{T}$ are a reminder that two of the terms in the full expansion of right side of Eq. (11) are singular at each of these points.

The effects shown in Fig. 3 reflect the trends seen in Fig. 2, the errors in the approximate formulae increasing with decreasing β and $\bar{T}$. It is interesting to note that for all barriers, the simple approximate formula Γ_{∞}^{II} is as good as the more general expression Γ_{∞}^{I} <u>wherever</u> the latter is reasonably accurate. For the larger barriers ($\beta \gtrsim 20$) this appears to include virtually all $\bar{T} > 1/\beta$. On the other hand, for all

barrier sizes, none of the approximate formulae are at all reliable for $\bar{T} < 1/\beta$.††

†† In addition to the results shown in Fig. 3, a calculation for $\beta = 80$ showed that its $\Gamma_\infty^I/\Gamma_{ex}$ curve has a minimum of 0.57 at $\beta\bar{T} = 0.84$, while for all $\beta\bar{T} \gtrsim 1.05$ it is within 1% of unity.

In addition to Γ_∞^I and Γ_∞^{II}, this includes Eqs. (7) and (10) in Bell's paper[2], which were suggested for use in this region. The former, proposed for $\bar{T} < 1/\beta$, would yield curves on Fig. 3 which would be identical to those for Γ_∞^I out to approximately their minima, and then would rise to infinity at $\beta\bar{T} = 1$. The latter, designed for $\bar{T} \approx 1/\beta$, would yield negative values of $\Gamma_\infty/\Gamma_{ex}$ for all $\bar{T}$ outside a very narrow interval about $\bar{T} = 1/\beta$, and even in this interval it is significantly less accurate than is Γ_∞^I.

To put the present results in perspective it is helpful to consider Caldin's[2] Table VII, which contains most of the reliable data on the dimensions of energy barriers for proton transfer reactions. For all of the cases presented there $\beta \gtrsim 30$, and the temperatures corresponding to $\beta\bar{T} = 1$ range between 130 and 250°K. Since most of the results were obtained using Γ_∞^{II} (Eq. (12)),[2] the experimental data for these cases must have corresponded to $\beta\bar{T} > 1$, and Fig. 3 suggests that their derived barrier parameter should be reasonably accurate. However, the present results clearly demonstrate that in those cases for which Eq. (11) had to be used (where $\beta\bar{T} \lesssim 1$), the reported barrier parameters are probably unreliable.

Another situation in which Bell's[7] approximate formulae have been used is in calculating tunneling corrections for the isotopic $H+H_2$ exchange reactions. Weston[15] fitted a parabola to the reaction path at the saddle point of a Sato[16] potential surface for collinear collisions, and used Bell's formulae[7] to estimate the tunneling through it. This parabolic barrier was 8.0 kcal/M high and had $\beta = 11.64$, so that $\overline{T} = 1/\beta$ corresponded to 340°K. Using the present method it was found that Weston's[15] predicted tunneling factors at 1000°K, 500°K, and 295°K are respectively 6% larger, and 6% and 35% smaller than the exact tunneling factors for his barrier.

APPROXIMATION OF BARRIERS BY ECKART AND PARABOLIC FUNCTIONS: RESULTS FOR $H+H_2$

The present section examines the appropriateness of approximating an actual barrier with a convenient analytic function, by considering the tunneling contribution to the simple hydrogen exchange reaction. Here the exact 1-Dim barrier is taken as the minimum potential path on the potential surface for collinear collisions. A number of treatments have previously estimated the amount of tunneling in this system using Eckart[3,9,17,18,19] or parabolic[9,15] approximations to the actual potential barrier.

The potential surface used here is the one reported by Shavitt, Stevens, Minn, and Karplus,[20] scaled by a factor of 0.89 as recommended by Shavitt.[18] The method of obtaining the present 1-Dim barrier from the low-energy path on this surface is described elsewhere.[10] Fig. 4

shows the actual energy barrier so obtained, curve A, and four approximations to it. Curves E_1 and P_1 are respectively Eckart and parabolic potentials with both the same height and curvature (second derivative) at the maximum as the "exact" barrier. Similarly, curves E_2 and P_2 are Eckart and parabolic barriers chosen to have the same height, and the same width at half maximum as the actual curve. The constant reduced mass used with these potentials is $\mu = M_H/3 = 0.33594$ amu. Fig. 5 shows the calculated tunneling factors for these potentials as a function of temperature; the total computer time required to generate curve A is less than one minute on an IBM-7094. The curves in Fig. 5 are labled as in Fig. 4, with the addition of curve S which represents the tunneling factors predicted by Shavitt,[18] who fitted an Eckart function to the actual barrier using different criteria than those used here. His potential had the same curvature at the maximum as the actual barrier, and was "selected by inspection to give a good fit to the ab initio barrier over as much of its upper part as possible." The barrier so obtained[18] is in good agreement with the actual one for $\bar{E} \gtrsim 0.7$, although it is only 0.41 as high; considering the latter fact, the agreement of curve S with curve A is quite surprising.

As might be expected, the present Eckart tunneling factors (curves E_1 and E_2) are closer to the exact values than are the parabolic results. However, it is apparent that none of the present approximate barriers yields tunneling factors that are really very good, especially at low temperatures. On the other hand, the manner in which the approximate results straddle curve A (in Fig. 5) suggests that their main source of error lies in the criteria used to fit the approximate barriers to

the actual one. This is confirmed by the fact that Shavitt's Eckart function[18] yielded tunneling factors in remarkable agreement with the present exact values, despite the fact that his barrier is only 0.41 as high as the actual one. Furthermore, it seems certain that further variation of the two free Eckart parameters could yield even better agreement with curve A. By comparison, it was found that no truncated parabola would yield tunneling in good agreement with curve A over the whole temperature range shown. The best fit of this sort (corresponding to $\beta \simeq 19$) had $\Gamma(T)$ values which were significantly too small at high temperatures and too large at low. Thus, while the tunneling factors for the $H+H_2$ case are insensitive to the nature of an approximating barrier except near its maximum, they are very sensitive to its shape in this region. In any case, it seems clear that exact numerical computations of $\Gamma(T)$ should be used whenever the shape of the barrier is known.

CONCLUDING REMARKS

A method has been presented for calculating the exact transmission probabilities and tunneling factors for any 1-Dim potential barrier. It has been used to determine the region of validity of Bell's[7] approximate expressions for the tunneling factors for truncated parabolic barriers. It has also been used elsewhere[10] to help correlate with theory some new experimental measurements of the relative rates of the exchange reactions $H + H_2$ and $H + D_2$.

It is apparent that the cases in which Bell's[7] formulae are appropriate are precisely those in which there is relatively little barrier transmission except at energies close to and above its maximum. This insensitivity of such results to the nature of the potential except

near its maximum is further illustrated by the remarkable success of Shavitt's[18] approximation for the $H+H_2$ tunneling, discussed in the preceeding section. This suggests that if experimental results may be accurately explained using Eqs. (11) or (12) for values of β and $\bar{T}$ for which these expressions accurately reflect the appropriate truncated parabola (e.g., $\beta \gtrsim 20$ and $\bar{T} > 1/\beta$), then the truncated parabola so obtained accurately approximates the shape and height of the actual 1-Dim potential barrier near its maximum.

The present quantitative confirmation of the validity of Eqs. (11) and (12) for large barrier (negligible tunneling at low energies) situations will be reassuring to experimentalists who have been interpreting their data using these expressions. Also, the present method offers a way of treating cases where tunneling is important at energies well below the barrier maximum, but for which the Eckart function results are not sufficient. However, one should remember that the whole of the present approach is based on the rather strong assumption that a multidimensional problem may be meaningfully represented in 1-Dim. The validity of this approximation has recently been examined by Truhlar and Kuppermann.[21]

ACKNOWLEDGEMENTS

This work was supported in part by National Aeronautics and Space Administration Grant NGL 50-002-001. The authors are also grateful to the National Research Council of Canada for support, and for the award of scholarships to two of us (R.J.L. and K.A.Q.). In addition, R.J.L. would like to thank Professor Richard B. Bernstein for his encouragement.

APPENDIX: Subroutine for Calculating Barrier Transmission Probabilities

A Fortran listing of the computer subroutine used for the determination of $\kappa(\bar{E})$ follows. It assumes that the potential and abscissa arrays were previously prepared such that $V(I) = B_y \bar{V}(y)$ for $y = X(I)$; similarly the energy E is $B_y \bar{E}$. The listing given utilizes the Numerov integration procedure; however, the RKG algorithm is given separately at the end and may be simply substituted for the statements from 26 to 50.

```
      SUBROUTINE PRMEAB(N,ISY,IWR,BY,H,ZZ,E,PBY,X,V)
C*** SUBROUTINE TO CALCULATE EXACT QUANTAL TUNNELLING PROBABILITY FOR
C    A PARTICLE IMPINGING ON A 1-DIMENSIONAL POTENTIAL POTENTIAL, V(X),
C    WITH A KINETIC ENERGY  E.  PERMEABILITY IS  PBY.
C*** ARRAY DIMENSION IS  N, AND  N2=N/2  CORRESPONDS ROUGHLY TO THE
C    BARRIER MAXIMUM.  X(IRM) CORRESPONDS TO REAGENTS AND  X(IRP) TO
C    PRODUCTS.  ( 1 .LE. IRM .LT. N2 .LT. IRP .LE. N )
C*** THE TWO LINEARLY INDEPENDANT SOLUTIONS, DENOTED  C AND  S, ARE
C    INTEGRATED SUMULTANEOUSLY.
C*** INCREMENT OF INTEGRATION IS  H
C*** IF(ZZ.GT.0.0), ZZ IS THE WKB CONVERGENCE CONDITION USED TO SELECT
C    THE INTEGRATION INTERVAL. IF(ZZ.LE.0.0) USE WHOLE INTERVAL.
C*** IF(ISY.GT.0) BARRIER IS SYMMETRIC ABOUT  X(N2), OTHERWISE NOT.
C*** IF(IWR.GT.0) WRITE PBY AND UNITARITY TEST, OTHERWISE NOT.
      DIMENSION  X(N),V(N)
      DOUBLE PRECISION  DS,DC,DEN,DS2,DS3,DC2,DC3,GKB,GK,F2
      N2=N/2
      IRM=1
      IRP=N
      IF(ZZ.LE.0.0) GO TO 26
C*** DETERMINE INTEGRATION INTERVAL END POINTS  IRM AND  IRP. ASSUMES
C    BARRIER MAXIMUM ROUGHLY AT  X(N/2)
      ND=20
      JD=+1
      M=(N-N2)/ND -2
      IR=N-M*ND
    6 DO 10 I=1,M
      IR=IR+JD*ND
      AR1=E-V(IR)
      AR2=E-V(IR-JD)
      IF((AR1.LE.0.0).OR.(AR2.LE.0.0)) GO TO 10
      SQ1=SQRT(AR1)
      SQ2=SQRT(AR2)
      TST=ABS(4.*(SQ1-SQ2)/(H*(SQ1+SQ2)**2))
      IF(TST-ZZ)12,12,10
   10 CONTINUE
      JD=-JD
      WRITE(6,601) TST,X(IR)
      IR=IR+JD
      IF(E-V(IR))99,99,16
   12 JD=-JD
      DO 14 I=1,ND
      IR=IR+JD
      SQ2=SQ1
      SQ1=SQRT(E-V(IR))
      TST=ABS(4.*(SQ1-SQ2)/(H*(SQ1+SQ2)**2))
      IF(TST-ZZ) 14,14,16
   14 CONTINUE
   16 IF(JD) 18,18,24
   18 IRP=IR+1
      IF(ISY) 22,22,20
   20 IRM=N-IR
      GO TO 26
   22 M=N2/ND-2
      IR=M*ND+1
      GO TO 6
```

```
   24 IRM=IR-1
C*** INTEGRATION USING NUMEROV ALGORITHM.  START AT PRODUCT BOUNDARY
C    CONDITION FOR TRANSMITTED WAVE.
   26 GI=V(IRP-1)-E
      H2=H**2
      HV=H2/12.
      FI=(1.-HV*GI)
      GKB=DSQRT(-GI)
      C1=DCOS(GKB*X(IRP))
      C2=DCOS(GKB*X(IRP-1))
      S1=DSIN(GKB*X(IRP))
      S2=DSIN(GKB*X(IRP-1))
      YC1=FI*C1
      YC2=FI*C2
      YS1=FI*S1
      YS2=FI*S2
      NINT=IRP-IRM-2
      J=IRP-1
      F1=H2*GI
C**** PERFORM ACTUAL NUMERICAL INTEGRATION TO GET PERMEABILITY HERE.
      DO 25 I=1,NINT
      J=J-1
      YC3=YC2+YC2-YC1+F1*C2
      YS3=YS2+YS2-YS1+F1*S2
      F1=H2*(V(J)-E)
      F2=1./(1.-F1/12.)
      C2=YC3*F2
      S2=YS3*F2
      YC1=YC2
      YC2=YC3
      YS1=YS2
   25 YS2=YS3
      YC3=YC2+YC2-YC1+F1*C2
      YS3=YS2+YS2-YS1+F1*S2
      F2=1./(1.-HV*(V(IRM+1)-E))
      DC3=YC3*F2
      DS3=YS3*F2
      DS2=S2
      DC2=C2
   50 GK=DSQRT(E-V(IRM+1))
C*** DECOMPOSE SOLUTIONS TO GET AMPLITUDE OF INCIDENT WAVE.
      DS=DSIN(GK*H)
      DC=DCOS(GK*H)
      DEN=4.*DS**2
      AI2=(DS2**2+DS3**2+DC2**2+DC3**2-2.*DC*(DS2*DS3+DC2*DC3) +
     1   2.*DS*(DC3*DS2-DC2*DS3))/DEN
      PBY=GKB/(GK*AI2)
      TSTERR=(GKB/GK-(DC3*DS2-DC2*DS3)/DS)/AI2
      IF(IWR.LE.0) GO TO 99
      EP=E/BY
      WRITE(6,603)EP,PBY,X(IRM),X(IRP),TSTERR
   99 RETURN
  601 FORMAT(1H0 5X 14HERROR ... TST= E10.3, 42H  GREATER THAN  ZZ AT EX
     1TREME BOUNDARY  X= F8.3)
  603 FORMAT(1H0 2X 7HAT  E = E12.6,23H ,  PERMEABILITY  K(E)= E13.7,
     1  18H  WITH LIMITS  X = F7.3, 4H AND F7.3, 24H . UNITARITY TEST ER
     2ROR= E10.4  )
      END
```

```
C*** INTEGRATION USING RUNGE-KUTTA-GILL ALGORITHM.  START AT
C    PRODUCT BOUNDARY CONDITION.
C*** DECOMPOSE SOLUTIONS TO GET AMPLITUDE OF INCIDENT WAVE.
   26 GKB=DSQRT(E-V(IRP))
      C1=DCOS(GKB*X(IRP))
      S1=DSIN(GKB*X(IRP))
      DC1= GKB*S1
      DS1=-GKB*C1
      I=IRP
C*** ACTUAL INTEGRATION LOOP BEGINS HERE
   30 S2=S1
      C2=C1
      DS2=DS1
      DC2=DC1
      QSA=H*DS2
      QCA=H*DC2
      HE=H*(E-V(I))
      QSB=-HE*S2
      QCB=-HE*C2
      S1=S2+QSA/2.
      C1=C2+QCA/2.
      DS1=DS1+QSB/2.
      DC1=DC1+QCB/2.
      CSA= H*DS1
      CCA= H*DC1
      I=I-1
      HE=H*(E-V(I))
      CSB=-HE*S1
      CCB=-HE*C1
      S1=S1+0.2928932*(CSA-QSA)
      C1=C1+0.2928932*(CCA-QCA)
      DS1=DS1+0.2928932*(CSB-QSB)
      DC1=DC1+0.2928932*(CCB-QCB)
      QSA=0.5857854*CSA+0.1213214*QSA
      QCA=0.5857854*CCA+0.1213214*QCA
      QSB=0.5857854*CSB+0.1213214*QSB
      QCB=0.5857854*CCB+0.1213214*QCB
      CSA= H*DS1
      CCA= H*DC1
      CSB=-HE*S1
      CCB=-HE*C1
      I=I-1
      S1=S1+1.7071068*(CSA-QSA)
      C1=C1+1.7071068*(CCA-QCA)
      DS1=DS1+1.7071068*(CSB-QSB)
      DC1=DC1+1.7071068*(CCB-QCB)
      QSA=3.4142146*CSA-4.1213214*QSA
      QCA=3.4142146*CCA-4.1213214*QCA
      QSB=3.4142146*CSB-4.1213214*QSB
```

```
      QCB=3.4142146*CCB-4.1213214*QCB
      CSA= H*DS1
      CCA= H*DC1
      HE= H*(E-V(I))
      CSB=-HE*S1
      CCB=-HE*C1
      S1=S1+CSA/6.-QSA/3.
      C1=C1+CCA/6.-QCA/3.
      DS1=DS1+CSB/6.-QSB/3.
      DC1=DC1+CCB/6.-QCB/3.
      IF((I-1).GT.IRM) GO TO 30
      DS2=S2
      DC2=C2
      DS3=S1
      DC3=C1
   50 GK=DSQRT(E-V(IRM+1))
C**** END OF SECTION PECULIAR TO RKG INTEGRATION PROCEDURE.
```

References

1. S. Glasstone, K. J. Laidler, and H. Eyring, The Theory of Rate Processes (McGraw-Hill, New York, 1941).
2. E. F. Caldin, Chem. Rev. 69, 135 (1969).
3. H. S. Johnston, Gas Phase Reaction Rate Theory (Ronald Press, New York, 1966).
4. C. Eckart, Phys. Rev. 35, 1303 (1930).
5. a) E. C. Kemble, The Fundamental Principles of Quantum Mechanics (McGraw-Hill, New York, 1937), §21j; b) L. D. Landau and E. M. Lifschitz, Quantum Mechanics-Non Relativistic Theory, 2nd Edition (Permagon Press, London, 1965), p. 176.
6. K. A. Quickert and D. J. Le Roy, J. Chem. Phys. 52, 856 (1970).
7. R. P. Bell a) Trans. Faraday Soc. 55, 1 (1959); b) the discussion in chapter 11 of The Proton in Chemistry (Cornell University Press, Ithaca, New York, 1959).
8. a) E. Merzbacher, Quantum Mechanics (John Wiley & Sons, New York, 1961), pp. 91-93; b) W. Kauzmann, Quantum Chemistry (Academic Press Inc., New York, 1957), pp. 195-198; c) A. S. Davydov, Quantum Mechanics, (Permagon Press, Toronto, 1965), §26; d) see also pp. 38-47 in Ref. 3.
9. D. J. Le Roy, B. A. Ridley and K. A. Quickert, Disc. Faraday Soc. 44, 92 (1967).
10. a) K. A. Quickert, Ph.D. Thesis, University of Toronto (1970) b) K. A. Quickert and D. J. Le Roy, to be published.
11. See, e.g., R. W. Hamming, Numerical Methods for Scientists and Engineers (McGraw-Hill, New York, 1962), p. 215.

12. a) J. W. Cooley, Math Computations 15, 363 (1961); b) J. K. Cashion, J. Chem. Phys. 39, 1872 (1963).

13. S. Gill, Proc. Cambridge Philosophical Soc. 47, 96 (1951).

14. R. J. Le Roy, K. A. Quickert, and D. J. Le Roy, University of Wisconsin Theoretical Chemistry Institute Report WIS-TCI-384 (1970).

15. R. E. Weston, Jr., J. Chem. Phys. 31, 892 (1959).

16. S. Sato, J. Chem. Phys. 23, 592 and 2465 (1955).

17. I. Shavitt, J. Chem. Phys. 31, 1359 (1959).

18. I. Shavitt, J. Chem. Phys. 49, 4048 (1968).

19. E. M. Mortensen, J. Chem. Phys. 48, 4029 (1968).

20. I. Shavitt, R. M. Stevens, F. L. Minn and M. Karplus, J. Chem. Phys. 48, 2700 (1968).

21. a) D. G. Truhlar, Ph.D. Thesis, California Institute of Technology (1970), b) D. G. Truhlar and A. Kuppermann, J. Chem. Phys. 52, 0000 (1970).

Figure Headings

Figure 1: Schematic potential barrier.

Figure 2: Ratios of approximate (κ_∞) to exact numerical (κ_{ex}) transmission probabilities for truncated parabolic barriers, as a function of the reduced energy $\bar{E}$. The barrier maxima correspond to $\bar{E} = 1$.

Figure 3: Ratios of approximate (Γ_∞) to exact numerical (Γ_{ex}) tunneling factors for truncated parabolic barriers. The solid curves were obtained by using Eq. (11) for Γ_∞, and the broken curves, Eq. (12). The breaks in the former for $\beta\bar{T} \leq 1$ correspond to the points at which pairs of terms in Eq. (11) blow up (i.e., where $1/\beta\bar{T}$ is an integer).

Figure 4: Comparison of actual theoretical 1-Dim potential barrier for collinear $H + H_2$ collisions (curve A) with analytic approximations to it. Curves P_1 and P_2 are truncated parabolas corresponding to $\beta = 14.74$ and 24.84, respectively, while curves E_1 and E_2 are Eckart functions, $V(x) = V_o/\cosh^2(x/a)$, with $a = 0.28$ and 0.38 Å respectively. E_1 and P_1 have the same curvature at the maximum as does curve A, while E_2 and P_2 have the same width at half maximum.

Figure 5: Tunneling factors for the potentials shown in Fig. 4, labelled in the same manner. The additional curve, S, is Shavitt's[18] Eckart function estimate of the tunneling for this system. The broken horizontal line lies at unity.

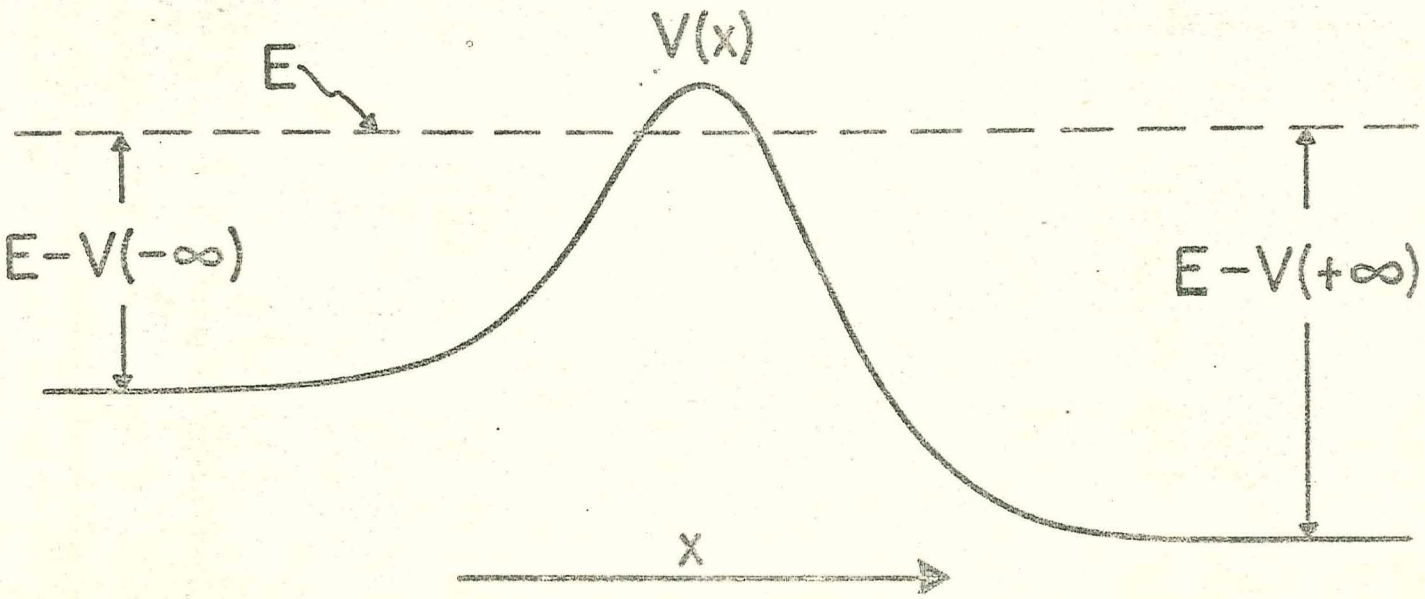

Figure 1

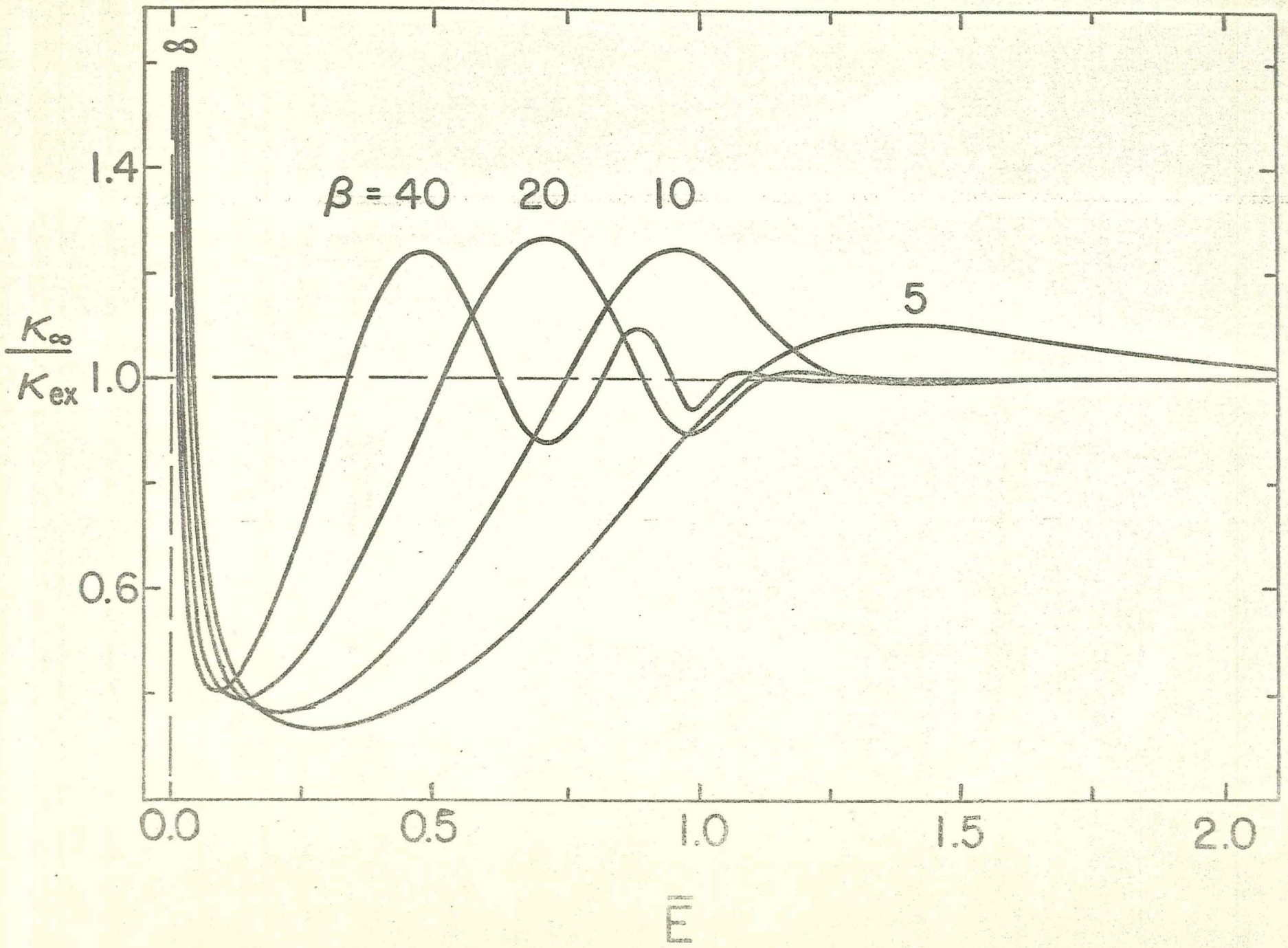

Figure 2

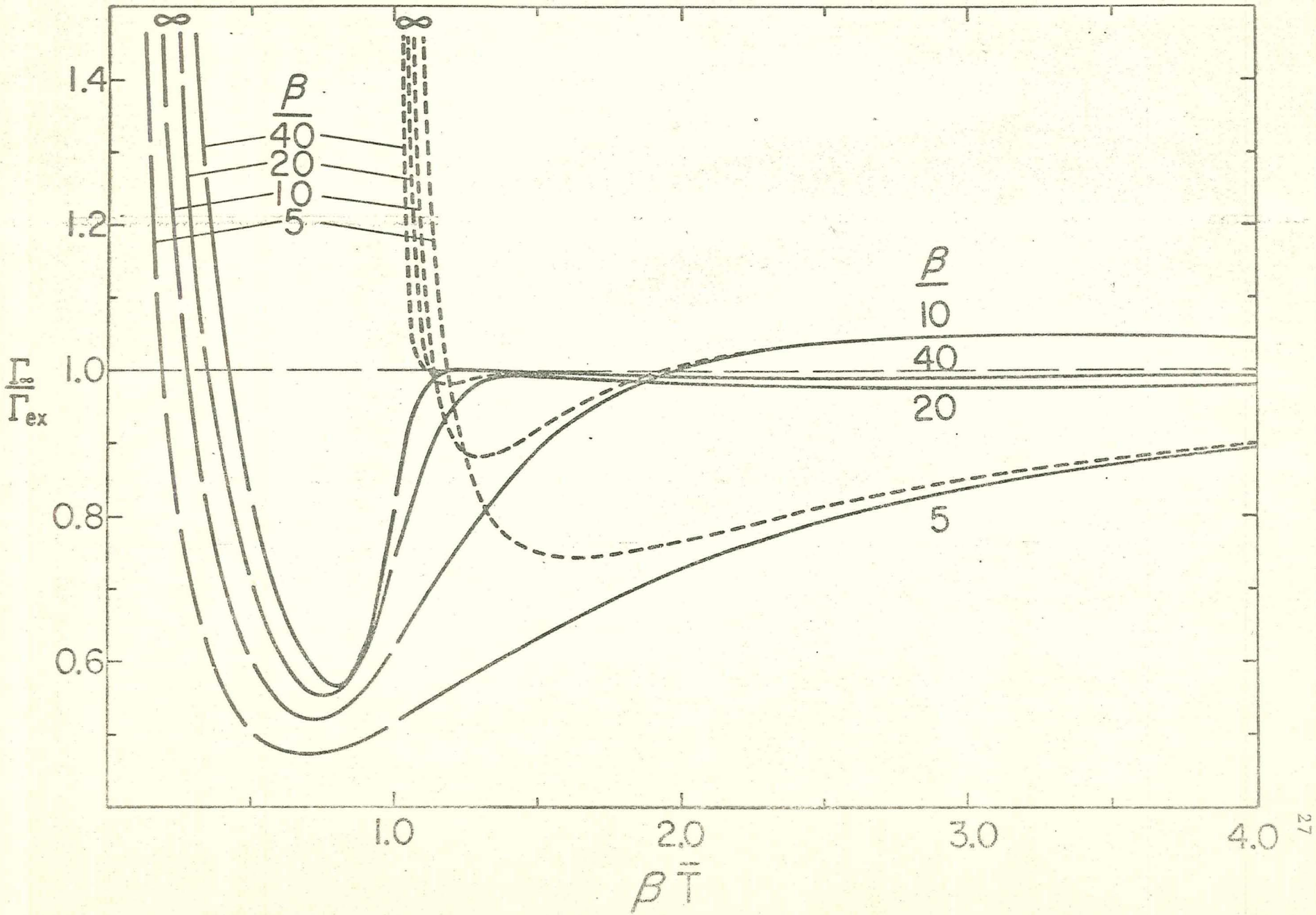

Figure 3

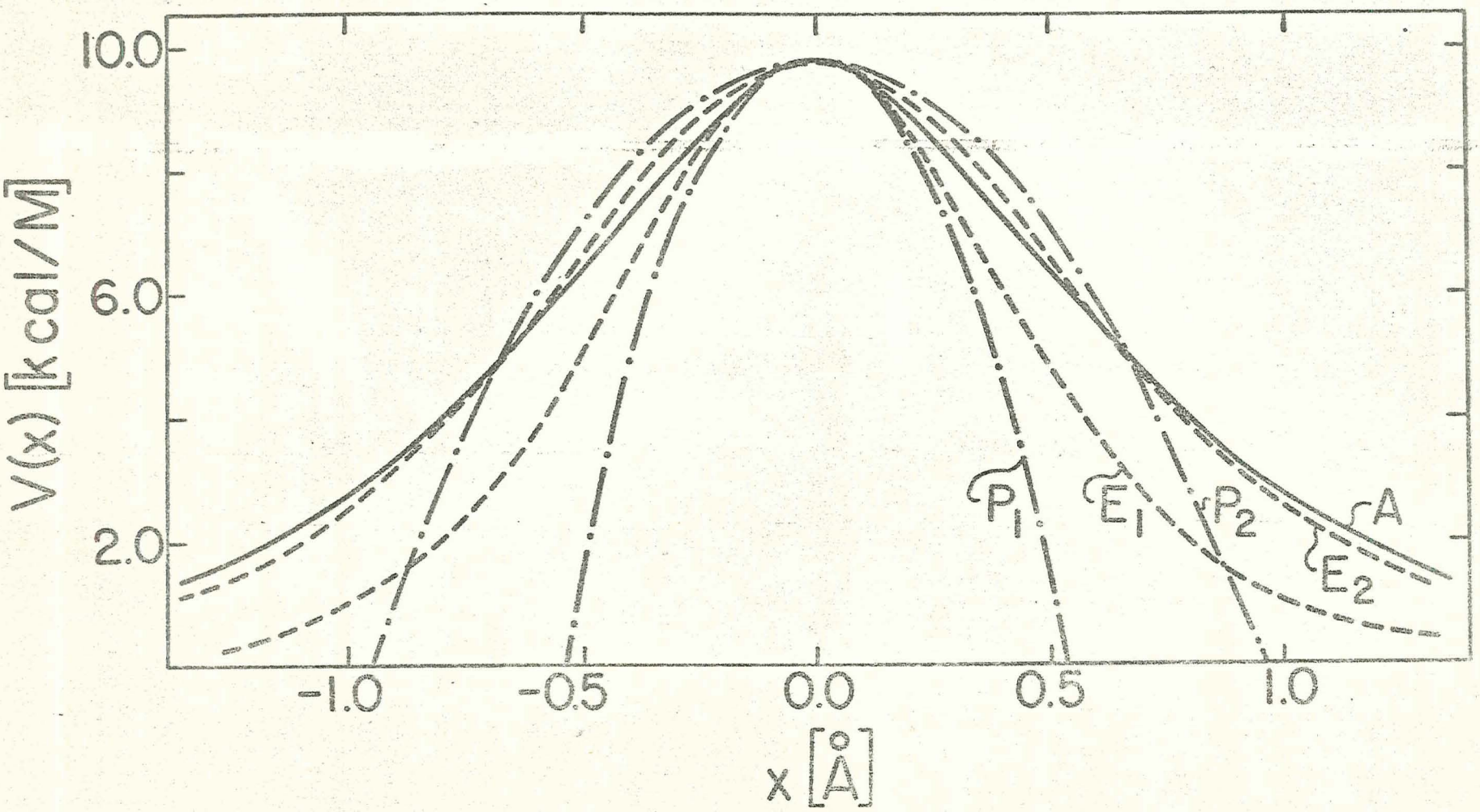

Figure 4

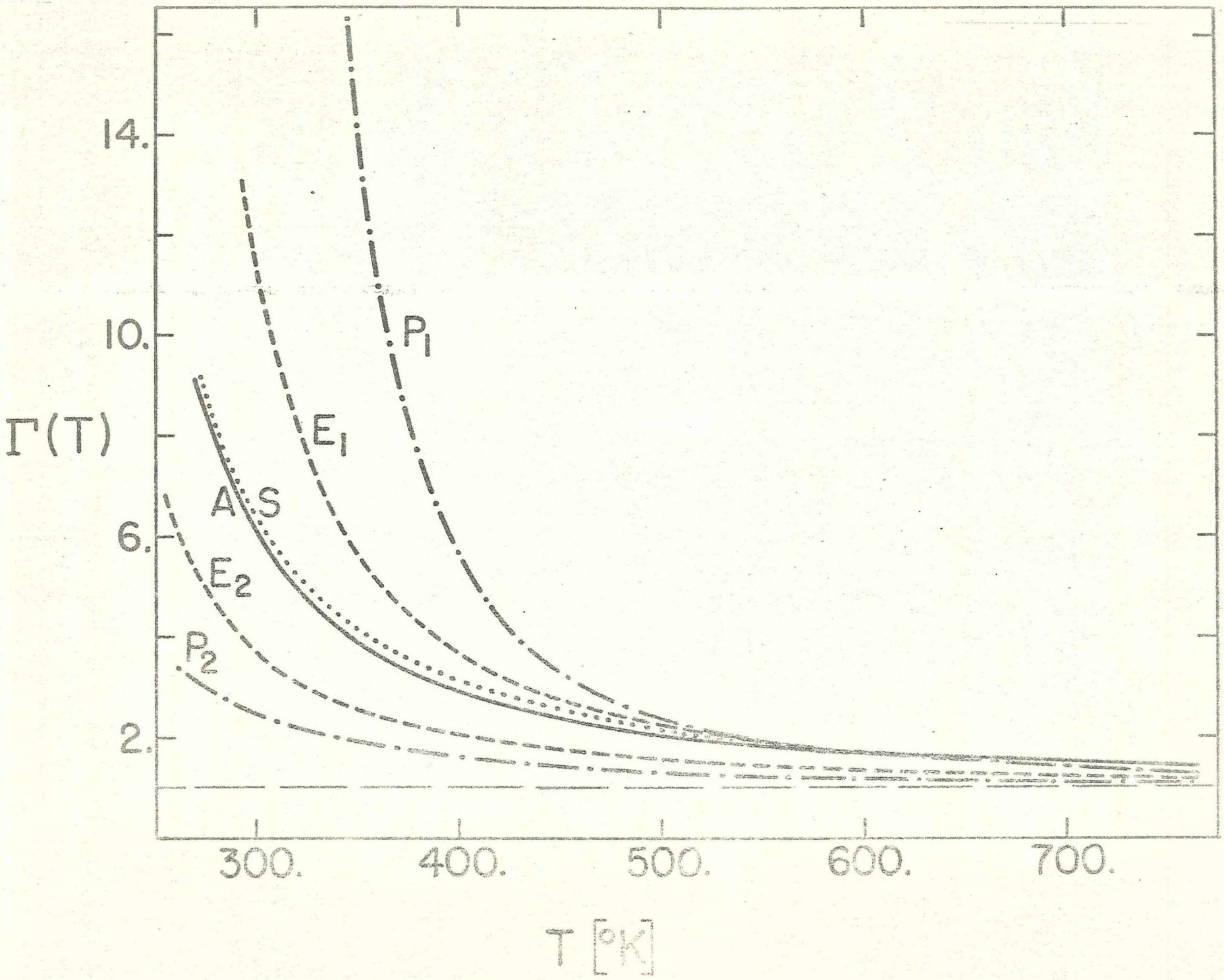

Figure 5